Biomech Model Mechanobiol (2011) 10:559–564
DOI 10.1007/s10237-010-0255-1

ORIGINAL PAPER

Quantification and significance of fluid shear stress field in biaxial cell stretching device

Mark S. Thompson · Stuart R. Abercrombie · Claus-Eric Ott · Friederike H. Bieler · Georg N. Duda · Yiannis Ventikos

Received: 3 March 2010 / Accepted: 1 September 2010 / Published online: 18 September 2010

Abstract A widely used commercially available system for the investigation of mechanosensitivity applies a biaxial strain field to cells cultured on a compliant silicone substrate membrane stretched over a central post. As well as intended substrate strain, this device also provides a fluid flow environment for the cultured cells. In order to interpret the relevance of experiments using this device to the in vivo and clinical situation, it is essential to characterise both substrate and fluid environments. While previous work has detailed the substrate strain, the fluid shear stresses, to which bone cells are known to be sensitive, are unknown. Therefore, a fluid structure interaction computational fluid dynamics model was constructed, incorporating a finite element technique capable of capturing the contact between the post and the silicone substrate membrane, to the underside of which the pump control pressure was applied. Flow verification experiments using 10-μm-diameter fluorescent microspheres were carried out. Fluid shear stress increased approximately linearly with radius along the on-post substrate membrane, with peak values located close to the post edge. Changes in stimulation frequency and culture medium viscosity effected proportional changes in the magnitude of the fluid shear stress (peak fluid shear stresses varied in the range 0.09–3.5 Pa), with minor effects on temporal and spatial distribution. Good agreement was obtained between predicted and measured radial flow patterns. These results suggest a reinterpretation of previous data obtained using this device to include the potential for a strong role of fluid shear stress in mechanosensitivity.

Keywords Cell culture · Computational fluid dynamics · Fluid shear stress · Mechanotransduction

M. S. Thompson (✉) · S. R. Abercrombie · Y. Ventikos
Institute of Biomedical Engineering, Department of Engineering Science, University of Oxford, Parks Road, Oxford OX1 3PJ, UK
e-mail: mark.thompson@eng.ox.ac.uk

M. S. Thompson
Biomedical Research Unit,
Nuffield Department of Orthopaedics,
Rheumatology and Musculoskeletal Sciences,
University of Oxford, Windmill Road, Oxford OX3 7LD, UK

F. H. Bieler · G. N. Duda
Julius Wolff Institute and Centre for Musculoskeletal Surgery,
Charité—Universitätsmedizin Berlin, Berlin, Germany

C.-E. Ott
Institute for Medical Genetics, Charité—Universitätsmedizin Berlin,
Berlin, Germany

1 Introduction

The mechanosensitivity of musculoskeletal tissue healing is well documented and presents a new paradigm for regenerative medicine in musculoskeletal tissue repair, whereby mechanical stimuli and pathways known to be mechanically regulated could be manipulated both pharmacologically and also physically to promote healing in patients where the endogenous repair response is insufficient. In order to follow this strategy, in vitro tools for stimulating cell culture have been employed to obtain the detailed knowledge of the biological response to mechanical excitation. The commercial availability of one such tool, the FX-4000T system (Flexcell Intern. Corp., Hillsborough, NC, USA), promotes a widespread repeatability of cell stimulation experiments; however, an essential additional pre-requisite for the establishment of a relevant body of knowledge in this area is precise characterisation of the mechanical stimuli experienced by the cultured cells.

Osteoblasts, producing mineralised matrix, have an essential role in fracture healing and are known to be mechanosensitive (Einhorn 1998); they have shown a differential response to stimuli magnitude in the synthesis of several factors important for bone healing (Chen et al. 2005; Liu et al. 2005; Tang et al. 2006; Bhatt et al. 2007).

Although many stimulation devices aim at providing a standardised substrate stretch, the cultured cells, covered by medium, are also subject to fluid flow. Studies on varying fluid flow and substrate stretch independently (Owan et al. 1997; Smalt et al. 1997) suggested that Osteoblast response was governed by fluid flow and not affected by substrate strain and strain rate magnitude, while simulations pointed to differing influences on cell deformation for substrate stretch and fluid flow (McGarry et al. 2005).

In order to resolve these issues and provide a framework for interpreting the results of stimulation experiments, it is essential to characterise both substrate and fluid shear stimuli for the FX-4000T device. Previous work from our group has demonstrated the existence of an area of membrane experiencing homogeneous, biaxial strains in BioFlex (Flexcell Intern. Corp., Hillsborough, NC, USA) well plates in the FX-4000T system (Bieler et al. 2009); however, the fluid flow environment in this device remains obscure.

The aim of this work was therefore, to provide a comprehensive, validated characterisation of the time-varying fluid shear stress field experienced by cells cultured in BioFlex wells in the FX-4000T device, including its spatial homogeneity and the effects of stimulation frequency and magnitude and of culture medium viscosity.

2 Materials and methods

2.1 Domain geometry

We represented a single BioFlex well in the FX-4000T system using a rectangular axisymmetric domain (radius 18.2 mm, depth 4.35 mm; dimensions from the manufacturer checked by repeated micrometer calliper measurements). Unstructured grids modelled the rigid post (radius 12.5 mm) and lip of the well; fully structured grids were used for the membrane (thickness 0.495 mm) and fluid, with predeformation of the fluid grid required in the off-post region to accommodate large deformations (Fig. 1). Fluid depth (2 mm) corresponded to the normal volume of cell culture medium in experimental protocols. The maximum Reynolds number was estimated at 230 indicating a laminar regime for flow.

This model was analysed using fluid structure interaction techniques within CFDACE+ (ESI CFD, Paris, France). The fluid analysis made use of the finite volume method, solving the incompressible and unsteady Navier–Stokes equations across each control volume (CV), utilising a second-order central differencing scheme in space. An algebraic multigrid method enhanced the solution speed through use of hierarchical grid resolutions (Lonsdale 1993). The behaviour of the substrate membrane was incorporated using the finite element method with the principle of virtual work (Zienkiewicz 1971), with second-order elements and frictionless contact with the underlying post. Mechanical testing of dog-bone specimens of Bioflex membrane provided an equivalent Young's modulus of 1.7 MPa, and a Poisson's ratio of 0.49 was assigned to the linear elastic material model of the membrane in CFD-ACE.

Time discretisation followed a second-order Crank–Nicholson scheme with a 0.005-s time step.

The fluid surface was modelled using a zero pressure boundary condition (a decision justified by the relatively low frequency and amplitude of the free surface oscillation), and a time-varying control pressure, modelling the action of the system pump, was applied to the lower surface of the off-post membrane.

2.2 Load cases

Modelling was first carried out by simulating a "base case" with a 20-kPa pressure wave at 1 Hz and standard culture medium viscosity (0.78 mPas at 37°C) (Bacabac et al. 2005a). Additional studies were performed with varying pressure wave frequency (2, 5 Hz) and magnitude (40 kPa), and also culture medium viscosity (20, 31 mPa s), simulating the addition of 0.1 and 0.2 wt% carboxymethylcellulose (CMC) (Kästner et al. 1997), was used to control medium viscosity in cell culture studies (Sen et al. 2002). A further study simulating a 1% CMC solution was carried out assuming non-Newtonian behaviour as described by the Ostwald de Waele equation (Ghannam and Esmail 1997).

2.3 Flow verification

The motion of an array of 10 μm diameter neutrally buoyant particles injected at 3 levels above the membrane (0.52, 1.04 and 1.56 mm) and at 6 radial positions (2, 3, 4, 5, 6 and 7 mm) was simulated by tracking an adequately large number of particles with identical properties, using a Lagrangian framework (as implemented within CFD-ACE+). Nominal diameter 10 μm (Duke Scientific, Palo Alto, CA) green fluorescent (508 nm) neutrally buoyant polystyrene microparticles dispersed in culture medium ($\sim 1 \times 10^6$ particles mL^{-1}) were injected during continuous operation of the FX-4000T at 0.5 Hz using a 0.1 mm syringe. Particle motion was followed from injection for 12 cycles using a vertically mounted digital SLR camera (D70, Nikon, Japan) with a bellows enlarging lens giving 2.3 μm/pixel at a capture rate of 3 Hz. The lens was adjusted to give a focal

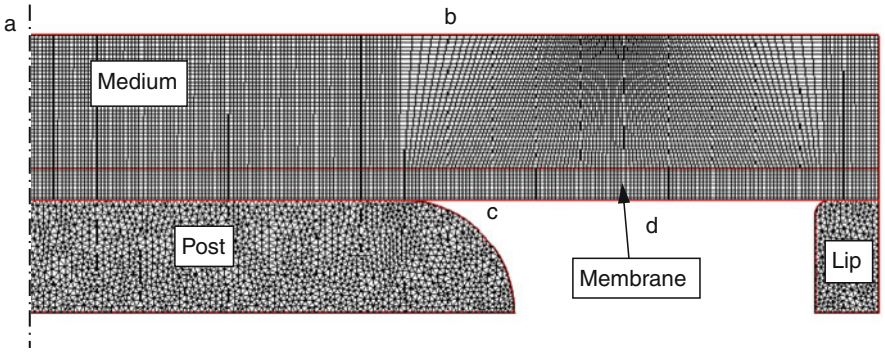

Fig. 1 Fluid structure interaction model: **a** axis of symmetry, **b** *upper* fluid boundary set to reference pressure, **c** contact modelled between membrane, post and lip, **d** applied pump pressure. Medium modelled as Newtonian fluid, density 1.0 g dm^{-3}, various viscosities, with a fully structured grid, pre-deformed in the off-post region. Post and lip provide rigid contact surfaces. Membrane modelled as an elastic material, $E = 1.7$ MPa, $\nu = 0.49$

plane lying approximately 1 mm from the membrane surface. The images were analysed using ImageJ and the ParticleTracker plug-in (Sbalzarini and Koumoutsakos 2005) to calculate resultant velocities per cycle.

3 Results

Grid independence was established at 60,000 CVs with a 4% maximum difference in membrane surface fluid shear stress on-post from a model with 100,000 CVs, while cycle independence was achieved with the second cycle.

A visualisation of radial velocity and membrane strain for the entire fluid structure interaction solution (Fig. 2) shows fluid moving in the off-post direction during the first part of the loading cycle (max 0.0036 m/s), while returning during the second half of the cycle (max 0.02 m/s). Off-post there is a substantial vertical component of fluid velocity, and the spatial gradient of this contributes to local membrane shear stresses; however, in the on-post region, the radial flow dominates. In agreement with our previous measurements (Bieler et al. 2009), tensile strain was uniform in the membrane remaining over the flat surface of the post and showed peak values at a radius of 9.8 mm, in the region of the curved edge of the post.

Under all conditions examined, the fluid shear stress at the surface of the membrane varied approximately linearly with radial position on-post throughout the stretch cycle (Fig. 3), with peak shear stresses occurring about 1 mm beyond the post edge.

A doubling of the modelled control pressure (from 20 to 40 kPa) increased on-post membrane strain from 3.8 to 6.7%, varying from the available machine calibration data but in agreement with image correlation measurements made with this device (Bieler et al. 2009). The peak fluid shear stress increased from 0.088 to 0.132 Pa and maximum vertical off-post membrane deflection increased from 1.4 to 1.9 mm, agreeing with measurements on the device. The cyclic shear stress variation with time was more symmetric at higher applied pressure.

Increasing the frequency of the applied control pressure (to 2 and 5 Hz) produced an approximately linear increase in shear stress magnitude (Fig. 4) with peak stresses of 0.172 and 0.424 Pa, respectively. Only small changes in time or spatial distribution of the shear stresses or membrane strains were noted. Increases in Newtonian viscosity to 20 and 31 mPas (0.1 and 0.2% CMC) produced approximately linear increases in shear stress magnitude (peak values 2.27, 3.52 Pa) with a very limited effect on time or spatial distribution (Fig. 5). Modelling in the non-linear regime corresponding to a 1% CMC solution predicted viscosities of up to 60 mPa s in the bulk medium but as low as 30 mPa s close to the membrane due to shear thinning with high strain rates and hence peak shear stresses of only 5.25 Pa.

The evaluation of computational predictions against tracked microsphere movement showed fair agreement on particle velocity across a range of radii (Fig. 6), especially when the uncertainty of particle insertion and depth is taken into account. All the velocities of particles in the simulated array fall within the envelope of velocities defined by the imaged microspheres and show similar increases with radius. Further, the magnitudes of predicted uniform membrane strains within a radius of 9.8 mm agree with previous measurements and models (Vande Geest et al. 2004; Bieler et al. 2009).

4 Discussion

The first ever fluid structure interaction simulations of the FX-4000T device presented here show that the membrane surface fluid shear stress is inhomogeneously distributed

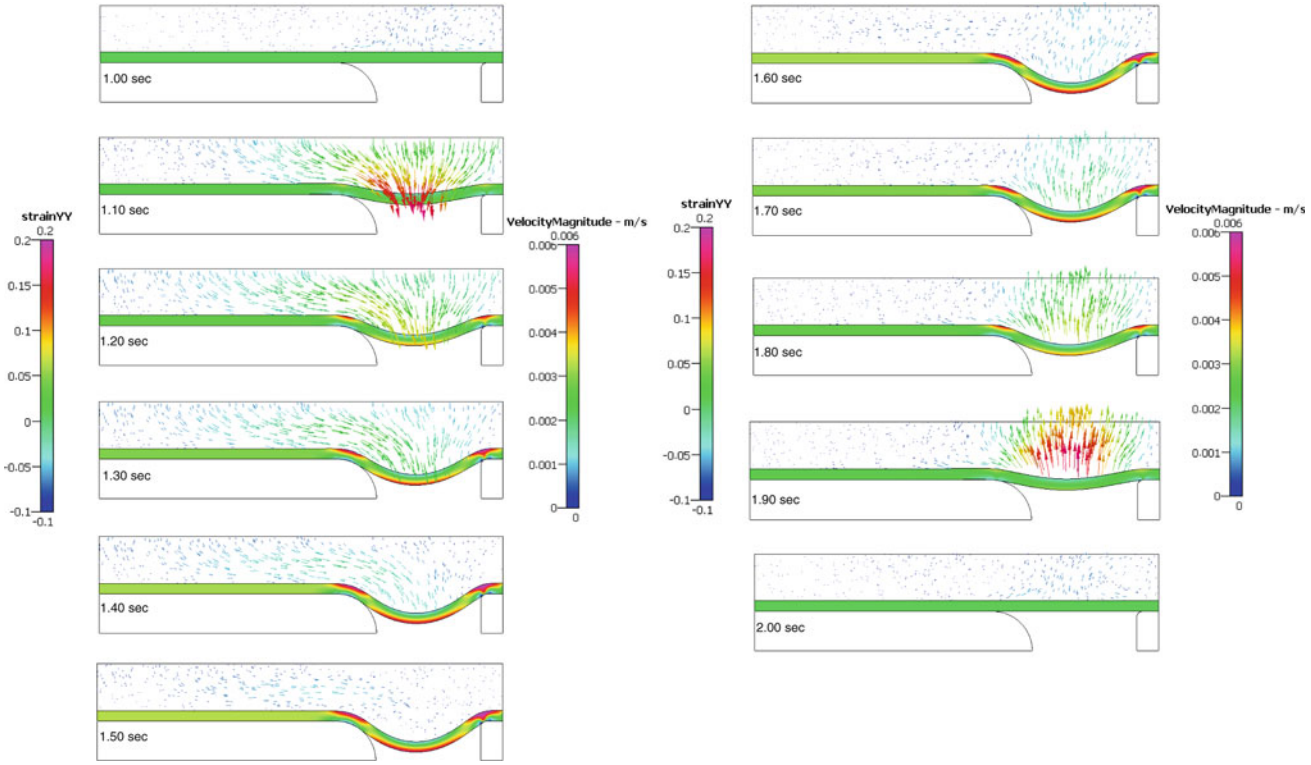

Fig. 2 Visualisation of fluid velocity and membrane strain for pump pressure 20 kPa, 1 Hz with culture medium viscosity 0.78 mPas

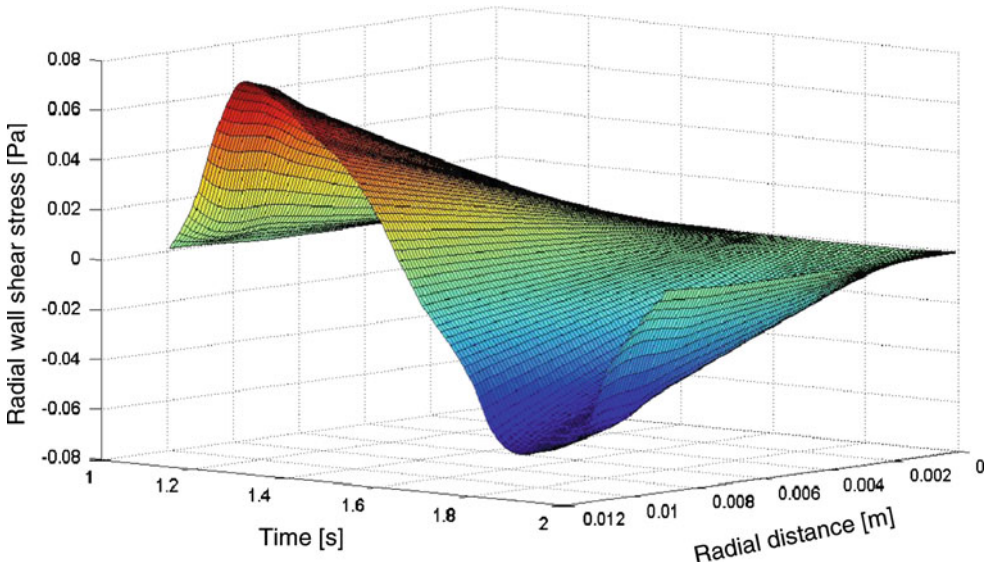

Fig. 3 Visualisation of radial shear stress distribution in on-post region—"base case"

with an approximate linear increase along an on-post radius. The shear stress magnitude varies linearly over the range 0.088–3.52 Pa with the frequency of applied stimuli and the viscosity of the culture medium (within the linear regime). These two parameters, together with the magnitude of the applied control pressure, have only a limited effect on the form of the shear stress distribution in space or time.

Previous fluid structure interaction models of a similar cell stimulating device, using the same principle of operation but lacking a central post, predicted maximum membrane shear stresses of 0.055 Pa occurring in 6 mm depth of fluid at an operating frequency of 1 Hz (Brown et al. 2000). The substantial difference in geometry also generated different spatial and temporal distributions of shear stresses,

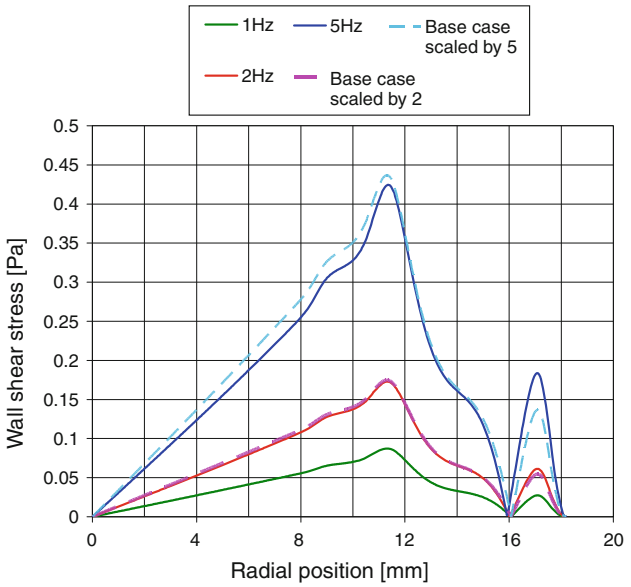

Fig. 4 Shear stress magnitude radial distribution variation with frequency at 15% of cycle time: comparison with proportionally scaled "base case" distribution

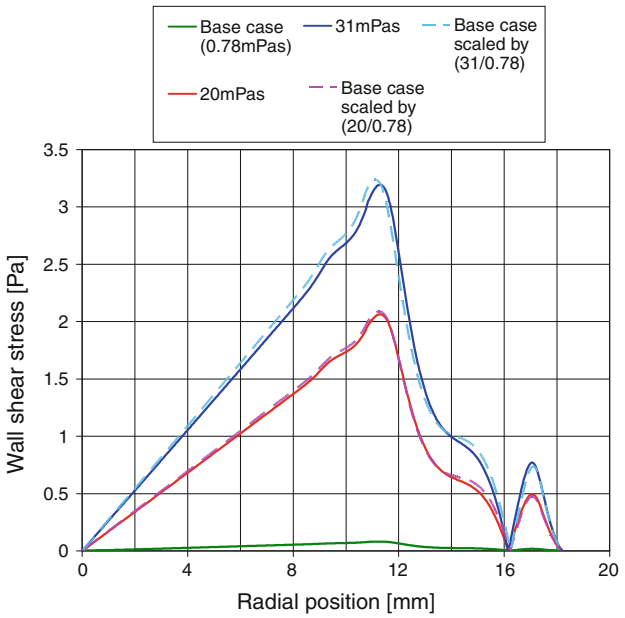

Fig. 5 Shear stress magnitude radial distribution variation with viscosity at 0.15 s: comparison with proportionally scaled "base case" distribution

though unfortunately only one simulation was reported in that study, so the effects of frequency, control pressure and medium viscosity cannot be compared.

The shear stress magnitude range predicted in this report for the FX-4000T system encompasses ranges previously reported to be important for bone cells (Pavalko et al. 1998; Bakker et al. 2001). Previous workers with this specific device have presented results in terms of a dependence on

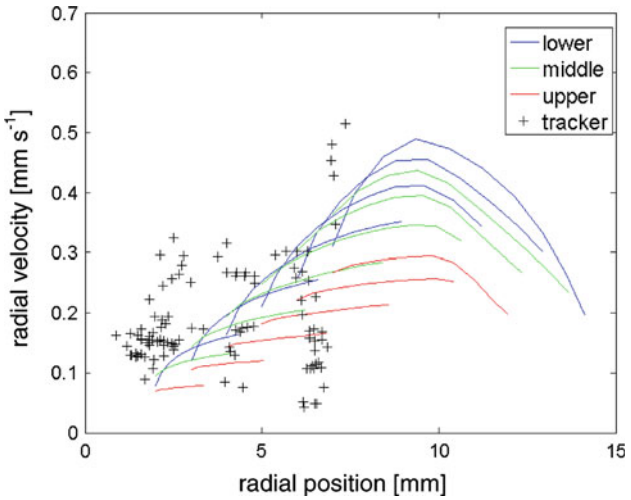

Fig. 6 Radial velocity against current radial position: comparison of CFD predictions (*solid lines*: lower, middle and upper rows in particle array) and experimental measurement (image-tracked fluorescent microspheres)

substrate strain, but their data are therefore, also consistent with a major role for fluid flow.

The predicted linear dependence of the shear stress magnitude on frequency leads to a quadratic dependence of shear stress rate on frequency. Bone cells have been reported to be sensitive to the time derivative of fluid shear stress (Jacobs et al. 1998; Bacabac et al. 2005b), and indeed strong responses to changes in stimulation frequency in the FX-4000T have been noted (personal communication).

Recent evidence suggests, due to the viscoelastic nature of the system, that membrane strain amplitude in these devices varies with frequency and waveform (Colombo et al. 2008) and with number of cycles (Bieler et al. 2009). Based on the outcome of varying the applied control pressure in our simulation, fluid shear stress is likely also to be affected by these issues.

The difficulty and computational cost in modelling fluid surface responses in a fluid structure interaction simulation led to the use of the zero pressure fluid surface boundary condition. This is a substantial simplification; however, its effects on shear stresses remote from this boundary are likely to be small as demonstrated by a Froude number of less than 0.08. A further assumption of axisymmetry was also made on grounds of the computational cost of full 3D simulations. Evidence for patterns of non-axisymmetric flow was provided by the fluorescent microsphere data; however, the radial component of the velocity used for the evaluation of the model was always largest.

Cells cultured on a 2D surface behave differently from cells cultured in 3D. Although it is possible to provide stimuli to cells in 3D microstructures in vitro, estimates of strain stimuli may be accurate only to within 50% and fluid shear

stress stimuli are often neglected (Baas et al. 2010). In order to advance knowledge of mechanotransduction and its role in bone maintenance, models that provide both accurate knowledge of mechanical conditions and a degree of physiological fidelity are required.

Our simulations demonstrate that the FX-4000T system may be used to investigate the effects of a range (0.09–5.2 Pa) of relevant shear stress magnitudes varying independently of the substrate strain. Unlike substrate strain, the shear stress is inhomogeneously distributed across the central post. Our results suggest that previous reports of dependence of bone cell response on substrate strain magnitude in this device should be reinterpreted to include a strong role for fluid flow.

Acknowledgments This research was supported by the John Fell OUP Research Fund, University of Oxford, by the Hans Jörg Wyss AO Medical Foundation and by the BMBF funded Berlin-Brandenburg Center for Regenerative Therapies. Claus-Eric Ott is supported by the Deutsche Forschungsgemeinschaft (DFG), Contract grant number: SFB 760. The authors are grateful to Dr M. Megahed for allowing the use of the CFD-ACE platform.

References

Baas E, Kuiper JH, Yang Y, Wood MA, El Haj AJ (2010) In vitro bone growth responds to local mechanical strain in three-dimensional polymer scaffolds. J Biomech 43:733–739

Bacabac RG, Smit TH, Cowin SC, van Loon JJWA, Nieuwstadt FTM, Heethaar R, Klein-Nulend J (2005a) Dynamic shear stress in parallel-plate flow chambers. J Biomech 38:159–167

Bacabac RG, Smit TH, Mullender MG, van Loon JJWA, Klein-Nulend J (2005b) Initial stress-kick is required for fluid shear stress-induced rate-dependent activation of bone cells. Ann Biomed Eng 33:104–110

Bakker AD, Soejima K, Klein-Nulend J, Burger EH (2001) The production of nitric oxide and prostaglandin E(2) by primary bone cells is shear stress dependent. J Biomech 34:671–677

Bhatt KA, Chang EI, Warren SM, Lin S, Bastidas N, Ghali S, Thibboneir A, Capla JM, McCarthy JG, Gurtner GC (2007) Uniaxial mechanical strain: an in vitro correlate to distraction osteogenesis. J Surg Res 143:329–336

Bieler FH, Ott CE, Thompson MS, Seidel R, Ahrens S, Epari DR, Wilkening U, Schaser KD, Mundlos S, Duda GN (2009) Biaxial cell stimulation: a mechanical validation. J Biomech 42:1692–1696

Brown TD, Bottlang M, Pedersen DR, Banes AJ (2000) Development and experimental validation of a fluid / structure-interaction finite element model of a vacuum-driven cell culture mechanostimulus system. Comput Methods Biomech Biomed Eng 3:65–78

Chen X, Macica CM, Ng KW, Broadus AE (2005) Stretch-induced PTH-related protein gene expression in osteoblasts. J Bone Miner Res 20:1454–1461

Colombo A, Cahill PA, Lally C (2008) An analysis of the strain field in biaxial flexcell membranes for different waveforms and frequencies. Proc Inst Mech Eng [H] 222:1235–1245

Einhorn TA (1998) The cell and molecular biology of fracture healing. Clin Orthop 355(suppl):S7–S21

Ghannam MT, Esmail MN (1997) Rheological properties of carboxymethyl cellulose. J Appl Polym Sci 64:289–301

Jacobs CR, Yellowley CE, Davis BR, Zhou Z, Cimbala JM, Donahue HJ (1998) Differential effect of steady versus oscillating flow on bone cells. J Biomech 31:969–976

Kästner U, Hoffmann H, Dönges R, Hilbig J (1997) Structure and solution properties of sodium carboxymethylcellulose. Colloids Surf A Physicochem Eng Asp 123(124):307–328

Liu X, Zhang X, Luo Z-P (2005) Strain-related collagen gene expression in human osteoblast-like cells. Cell Tissue Res 322:331–334

Lonsdale RD (1993) An algebraic multigrid solver for the navier-stokes equations on unstructured meshes. Int J Num Meth Heat Fluid Flow 3:3–14

McGarry JG, Klein-Nulend J, Mullender MG, Prendergast PJ (2005) A comparison of strain and fluid shear stress in stimulating bone cell responses—a computational and experimental study. FASEB J 19:482–484

Owan I, Burr DB, Turner CH, Qui J, Tu Y, Onyia JE, Duncan RL (1997) Mechanotransduction in bone: osteoblasts are more responsive to fluid forces than mechanical strain. Am J Physiol 273:C810–C815

Pavalko FM, Chen NX, Turner CH, Burr DB, Atkinson S, Hsieh Y-F, Qiu J, Duncan RL (1998) Fluid shear-induced mechanical signaling in MC3T3-E1 osteoblasts requires cytoskeleton-integrin interactions. Am J Physiol Cell Physiol 275:1591–1601

Sbalzarini IF, Koumoutsakos P (2005) Feature point tracking and trajectory analysis for video imaging in cell biology. J Struct Biol 151:182–195

Sen A, Kallos MS, Behie LA (2002) Expansion of mammalian neural stem cells in bioreactors: effect of power input and medium viscosity. Dev Brain Res 134:103–113

Smalt R, Mitchell FT, Howard RL, Chambers TJ (1997) Induction of NO and prostaglandin E2 in osteoblasts by wall-shear stress but not mechanical strain. Am J Physiol 237:E751–E758

Tang L, Lin Z, Li Y-M (2006) Effects of different magnitudes of mechanical strain on osteoblasts in vitro. Biochem Biophys Res Commun 344:122–128

Vande Geest JP, Di Martino ES, Vorp DA (2004) An analysis of the complete strain field within Flexercell(TM) membranes. J Biomech 37:1923–1928

Zienkiewicz OC (1971) The finite element method in engineering science. McGraw Hill, New York